

# Zig-Zag Wanderer: Towards Adaptive Tracking of Time-Varying Coherent Structures in the Ocean

Dhanushka Kularatne<sup>1</sup>, Ryan N. Smith<sup>2</sup> and M. Ani Hsieh<sup>1</sup>

**Abstract**—Similar to the atmosphere, coherent structures, e.g., fronts, exist in the ocean. These frontal structures are known to be highly productive, supporting the whole spectrum of marine life. Ocean fronts are dynamic in time and space, and are a key component to a comprehensive knowledge of ocean dynamics and aquatic ecosystems in relation to climate change. However, dynamic features such as fronts are difficult to study through conventional oceanographic techniques. In this paper, we build upon our previous work in sampling and tracking an ocean front based on predictions and/or priors. Specifically, given a prior (that may not be accurate or up-to-date) we present and experimentally validate a method for an autonomous surface or underwater vehicle to plan a mission and adapt this mission on-the-go to track a dynamic, but coherent, structure. Experimental results using a novel indoor testbed, capable of creating controllable fluidic features in an indoor laboratory setting, are presented. These results demonstrate that the vehicle is able to adapt its path to follow a desired, time-varying contour.

## I. INTRODUCTION

Ocean frontal zones are narrow bands of locally intensive physical gradients characterized by enhanced circulation and biological productivity. These systems divide broader areas with different water masses, vertical structure, or fluid dynamics. A front can be observed or detected via changes in multiple environmental properties (e.g., temperature, nitrate, salinity, etc.) [1]. However, precise study of these features has been a persistent challenge in ocean science as they occur across a variety of spatial scales; along-frontal scales of 1 km to 10,000 km, cross-frontal scales of 10 m to 100 km, and vertical scales of 10 m to 1000 m. Additionally, ocean fronts vary temporally on scales ranging from a few hours to a few weeks and even longer, e.g., the Kuroshio Front of the eastern coast of Japan. Given these challenges, ocean fronts cannot be studied through conventional oceanographic techniques [2], and a reliable model of the structure and behavior of fronts does not yet exist.

Current characterization and sampling methods for ocean fronts involve heuristics based on ship-based and remotely sensed measurements, e.g., [3], [4]. These heuristics inform oceanographers for sampling the different water masses that occur across and within the frontal boundaries. This is a difficult task and results in very sparse sampling when

conducted from large, manned vessels. To this end, it is of interest to examine the use of autonomous vehicles to provide a cost-effective and sustainable approach to sample these dynamic features at high spatial and temporal resolution for the purpose of developing models, both physical and biological. Additionally, there is also interest to determine the viability of using transport controlling ocean fronts, e.g. Lagrangian coherent structures (LCS) [5], which divide the flow field into dynamically distinct regions, as reduced-order models for predicting ocean dynamics. To develop such models, we must first gather enough information to begin to characterize these dynamic features in the flow field at multiple spatiotemporal scales. The challenges in data collection to support such model development are twofold: 1) translating existing oceanographic heuristics into features comprehensible by a robot, and 2) the ability to correctly identify such characterizing features in an environment with significant noise.

In this paper, we build on our previous work [6] and present a systematic experimental validation of an autonomous ocean front sampling and tracking strategy for a single autonomous surface vehicle (ASV) or an autonomous underwater vehicle (AUV). Given a prior (that may not be accurate or up-to-date), we present a systematic validation of an extension of the method presented in [6] which allows an ASV/AUV to plan a mission and adapt this mission on-the-go to track a dynamic front. Specifically, we present experimental results for the proposed sampling and tracking strategy that were conducted using a novel experimental testbed that is capable of creating controllable fluidic features in an indoor laboratory setting. These results show the vehicle's ability to adapt its path to follow a desired contour.

The structure of the paper is as follows: We briefly summarize related work in Section II. The modified sampling and tracking strategy is presented in Section III and the experimental methodology is presented in IV. A summary of the experimental results is presented in Section V. We conclude with a discussion of experimental insights and directions for future work in Section VI.

## II. RELATED WORK

Robotic platforms hold the promise of a revolution in ocean sampling. Considerable study has been reported on control design for AUVs for adaptive ocean sampling and coordinated control of multi-vehicle systems, e.g., [7]–[12]. Applications of ocean sampling techniques for AUVs are discussed in [9], [10], [13], [14], with ocean front perception and detection specifically addressed in [1], [7], [8], [15],

This work was supported by the Office of Naval Research (ONR) Award No. N000141310731.

<sup>1</sup>Dhanushka Kularatne and M. Ani Hsieh are with the SAS Laboratory, Mechanical Engineering & Mechanics Department, Drexel University, Philadelphia, PA 19104, USA {dnk32, mhsieh1}@drexel.edu

<sup>2</sup>Ryan N. Smith is with the Department of Physics and Engineering, Fort Lewis College, Durango, CO 81301, USA rnsmith@fortlewis.edu

[16]. Ocean front detection and characterization has been extensively studied without in situ robotics through satellite remote sensing [3], [4], [17]. These algorithms provide the foundation for the heuristics (priors) of robot comprehensible features.

To address adaptation, researchers have implemented human-in-the-loop solutions; static paths are created and alternative static paths are generated by domain experts after analyzing collected data [18]–[20]. These methods have their advantages, however we are interested in enabling decision making for path adaptation on-board the vehicle. Some results have implemented information-based metrics and machine learning to optimally determine a path or sensor placement based on reduction of overall covariance of the scalar field in question. Recent work in [7], [8] begins to address the issue of on-board decision making and adaptation, but approaches the problem from a multiple underwater vehicle point-of-view, with constraints on communication among the fleet.

Similar work in cooperative boundary tracking for robotic teams, which relies on one-dimensional (1D) parameterizations include [21], [22] and [23], [24] for static and time-dependent cases respectively. Formation control strategies for distributed estimation of level surfaces, scalar fields, and transport controlling features in the ocean are presented in [25]–[27]. These works leverage the spatio-temporal sampling capabilities of a team of robots where real-time tracking of ocean frontal features is accomplished by fusing multiple measurements obtained on opposite side of the front. Different from these work, this work focuses on the development and validation of a sampling and tracking strategy for a single autonomous surface or underwater vehicle. Here, we enable in situ robotic adaptation to environmental conditions for a single vehicle based on real-time measurements for targeted sampling of ocean fronts.

### III. ALGORITHM DESIGN

The objective of this work is to develop and validate an adaptive sampling and tracking strategy for a single AUV/ASV. The algorithm presented in this paper consists of two main components. The first is to generate an initial path for the AUV/ASV to traverse the front, based on a prior characterization of the front. This initial path is generated as a zig-zag pattern with a pre-defined swath width. The next part of the algorithm uses this initial path along with actual front locations determined in situ by the AUV/ASV to adaptively generate subsequent waypoints for the AUV/ASV to track the frontal structure. We only utilize the first few waypoints of the initial path, until two front locations are detected, to initialize AUV/ASV on the front; the remaining waypoints are adaptively determined based on in situ data while tracking the time-varying front. The motivation for this method comes from the technique presented in [4], which presents a front-following algorithm for remotely sensed data. Here, we attempt to adapt this heuristic based on static data into an adaptive planning algorithm that can be executed in situ .

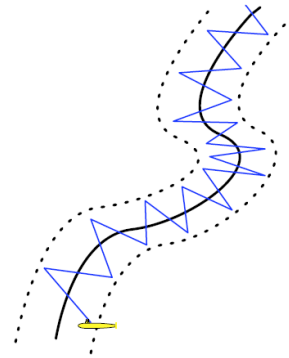


Fig. 1: Initial path generation for a specified front

#### A. Initial Path Generation

The same methodology used in [6] is used to generate the initial path. The AUV/ASV is provided with an estimate of the front location based on observations made by remote sensing agents (HF radar, UAV, satellite, etc. ). This estimate is used to generate a zig-zag path with a pre-defined swath width that traverses the estimated front. The swath width is based on the hyperbolic tangent function assumption proposed in [4] and is additionally adjusted from predictive models to compensate for the movement of the front near the initialization location. As shown in Fig. 1, the candidate waypoints for the zig-zag path are along the dashed lines located a distance of one half of the pre-defined swath width on either side of the prior observation. Interested readers are referred to [6] for more information on the generation of the initial path.

#### B. Adaptive Path Generation

In [6], the location of the frontal boundary is predicted by fitting a cubic spline to the previously gathered data. After the AUV/ASV has navigated through four waypoints of the initial path, the next front location is predicted using the three previously detected front locations. This predicted front location is used to compute the next waypoint for the AUV/ASV. The main difference in the algorithm presented in this paper is that the frontal boundary is predicted using a linear projection rather than a cubic spline. The main reason for this modification is the assumed time scale of the frontal boundary dynamics. Even if a complicated projection method is used to predict the next front location, there is no guarantee that the time scale of the front is captured by the more complex projection method.

At the start, the AUV/ASV navigates along the initial zig-zag path generated based on the prior, until it detects two frontal crossings. Once two consecutive front locations,  $f_n$  and  $f_{n-1}$ , have been detected, the AUV/ASV estimates the next location of the front  $\tilde{f}_{n+1}$ , using a linear projection. In addition, once the front is crossed, the current destination waypoint  $p_n$  is recalculated to ensure that the vehicle does not travel too far beyond the front. The estimated front location and the current waypoint are then used to generate

the next waypoint  $p_{n+1}$  for the AUV/ASV.

---

**Algorithm 1** Adaptive Path generation

---

- 1: **if**  $f_n$  located before reaching  $p_n$  **then**
  - 2:    $\tilde{f}_{n+1} = f_n + (f_n - f_{n-1}) \times a$
  - 3:    $p_n = f_n + (f_n - p_{n-1}) \times b$
  - 4:    $p_{n+1} = \tilde{f}_{n+1} + (\tilde{f}_{n+1} - p_n) \times c$
  - 5: **else**
  - 6:   *terminate*
- 

In the algorithm, the constants  $a$ ,  $b$  and  $c$  determine how far  $\tilde{f}_{n+1}$ ,  $p_n$  and  $p_{n+1}$  are projected forward respectively.  $c$  needs to be set at a sufficiently large value to ensure that the sensing agent crosses the front in the next path segment. Even though this makes the next projected waypoint far away from the predicted front, it does not impact the performance of the tracking strategy since this waypoint is recalculated when the next front location is detected. The algorithm is terminated if a front location is not found before reaching  $p_n$ .

#### IV. EXPERIMENTAL METHODOLOGY

To evaluate the sampling and tracking strategy using an experimental robotic platform, we employ our multi-robot Coherent Structure Testbed (mCoSTe) [28]. In these experiments, we use the proposed algorithm to track velocity fronts in a flow field. However, it must be noted that the algorithm is equally applicable for tracking other types of fronts with appropriate sensing agents.

##### A. Experimental Setup

The mCoSTe is an indoor laboratory experimental testbed that consists of three flow tanks and a fleet of two types of micro-autonomous surface vehicles: the mASV and the mASVf. The mASVs are differential drive surface vehicles equipped with a micro-controller board, XBee radio module, and an inertial measurement unit (IMU). The vehicles are approximately 12 cm long and have a mass of about 45 g each. The mASVfs are similar to the mASVs except they are equipped with onboard flow sensors capable of measuring the relative speed and direction of the local flow field. Flow sensors comprise of high resolution rotary encoders connected to aluminum rods that extend into the water. Each mASVf is approximately 15 cm long and has a mass of about 110 g. Localization for both the mASVs and the mASVfs is provided by an external motion capture system. Fig. 2 shows examples of the mASVs and mASVfs.

In addition to the vehicles, we also employed one of the mCoSTe's experimental flow tanks: the Multi-Robot (MR) Tank which is  $3 \times 3 \times 1$  m<sup>3</sup> in size. The MR tank is pictured in Fig. 4. The MR tank is designed to accommodate the operation of several mASVs and mASVfs and is able to create time-independent flow fields that exhibit kinematic and transport features similar to those observed in the ocean [28]. The flows in the tanks are patterned after the wind-driven double gyre flow model which is often used to describe large scale recirculation in the ocean [29]. For additional details

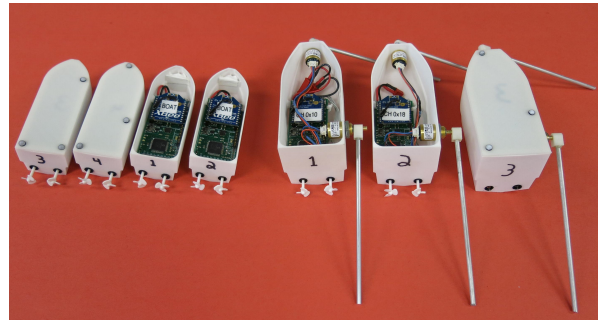


Fig. 2: Examples of the two types of ASVs used in the experiment. Shown on the left are the mASVs and on the right are the mASVfs.

of the various components of the mCoSTe and the quality of the flows that can be created using the mCoSTe, we refer the interested reader to [28] for additional details.

##### B. Experimental Methodology

To evaluate the feasibility of the proposed algorithm in tracking velocity fronts using the mCoSTe, we use an mASV and an mASVf in the MR tank (see Fig. 2). The first set of experiments carried out to test the algorithm uses an mASV as the front tracking agent. Since mASVs do not have onboard flow sensing capabilities, artificial sensor outputs are generated for each mASV to simulate the flow in the tank. To make the measurements more realistic, noise is added to the artificial sensor outputs. This methodology allowed us to evaluate the algorithm on various flow fields which are not easily realizable in the experimental tank. The next set of experiments use the mASVf to track an actual front in the tank.

In all the experiments, points on the velocity fronts are characterized by having near zero flow velocities. Therefore, while crossing a front, the mASVs and the mASVfs are set up to detect periods where the measured flow velocity is below a specified threshold. The median point within this period is selected as the front location.

We considered the following scenarios in our experimental evaluation.

1) *Case 1a:* A *time-invariant* flow field was considered in which the  $x$  component  $V_x$  and the  $y$  component  $V_y$  of the flow velocity at a point  $(x, y)$  is given by

$$V_x = \frac{d\psi}{dx} \quad (1a)$$

$$V_y = \frac{d\psi}{dy} \quad (1b)$$

$$\psi = -[y - A \sin(\omega_b x)]^2 \quad (1c)$$

where  $A$  is the amplitude of the created front and  $\omega_b$  is the spatial frequency of the front. An mASV was used to track this simulated front in the MR tank.

2) *Case 1b:* Similar to Case 1a, but with zero mean Gaussian noise, with standard deviation  $\sigma = \sqrt{2I}$  with noise intensity  $I$ , added to the velocity measurements to simulate

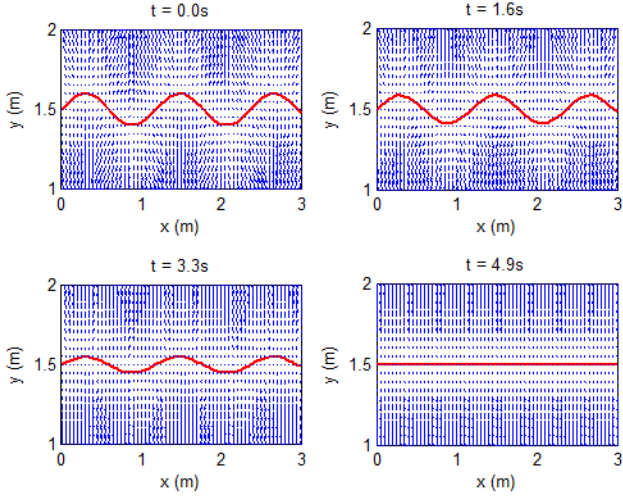


Fig. 3: Time varying velocity front with  $A = 0.1$ ,  $\omega_b = \frac{1}{6\pi}$ ,  $\omega_m = \frac{1}{\pi}$  and  $I = 0$

measurement noise. The experiment was repeated for  $I = 0.01$  and  $I = 0.05$ .

3) *Case 2:* A periodic flow field was considered where the  $x$  component  $V_x$  and the  $y$  component  $V_y$  of the flow velocity at a point  $(x, y)$  at time  $t$  is given by

$$V_x = \frac{d\psi}{dx} + \eta_x \quad (2a)$$

$$V_y = \frac{d\psi}{dy} + \eta_y \quad (2b)$$

$$\psi = -[y - A \cos(\omega_m t) \sin(\omega_b x)]^2 \quad (2c)$$

Terms in (2) have identical meanings as (1) with  $\eta_x$  and  $\eta_y$  representing the noise components and  $\omega_m$  representing the temporal frequency of the front created. The experiment was repeated for  $I = 0$ ,  $I = 0.01$  and  $I = 0.05$ . The underlying flow field with  $A = 0.1$ ,  $\omega_b = \frac{1}{6\pi}$ ,  $\omega_m = \frac{1}{\pi}$  and  $I = 0$  is shown in Fig. 3. An mASV was used in the MR tank to track this simulated time varying flow field.

4) *Case 3:* Actual flow data obtained from the MR tank. A flow field was created in the MR tank with four rotating cylinders, each having a diameter of 10 cm and rotating in the counterclockwise direction at an approximate speed of 4 rev/s as shown in Fig. 4. This created a front with near zero velocity through the middle of the tank. It must be noted that the created front was time varying due to inherent noise and asymmetries in the system. A mASV was deployed to measure and track the velocity fronts generated in the flow.

## V. RESULTS

For each of the scenarios described in section IV, multiple trials were run and the results were recorded. To evaluate the performance of the algorithm, the mean square error (MSE) given by

$$MSE = \frac{\sum_{i=1}^n f_i - \bar{f}_i}{n} \quad (3)$$

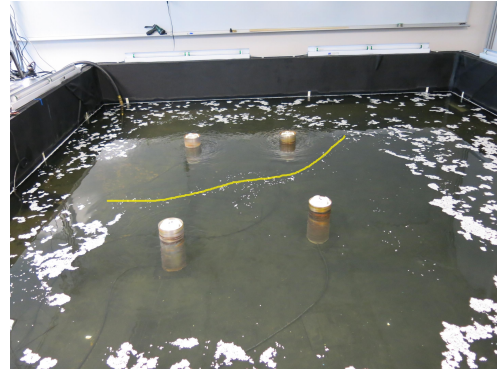


Fig. 4: MR tank with a velocity front created with four rotating cylinders.

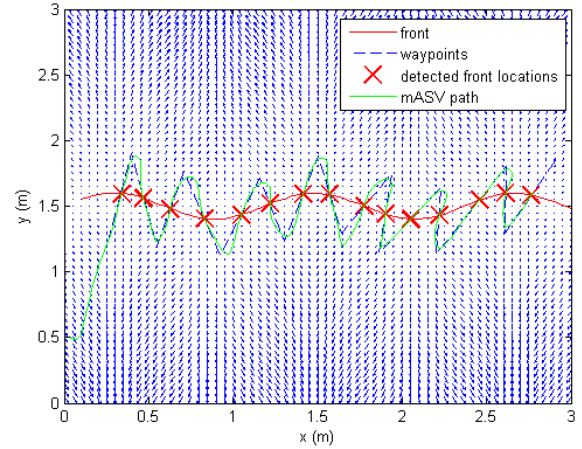


Fig. 5: Tracking a time-invariant velocity front in the absence of measurement noise

was used. In (3),  $f_i$  is the  $i^{th}$  detected front location,  $\bar{f}_i$  is the actual location of the  $i^{th}$  front location and  $n$  is the total number of front locations detected.

1) *Case 1a:* A flow field generated by (1) with parameters  $A = 0.1$  and  $\omega_b = \frac{1}{6\pi}$  was used in this experiment. Fig. 5 shows the results when no measurement noise is considered. It can be observed that the front locations are detected very accurately in the absence of measurement noise.

2) *Case 1b:* In this experiment, noise was added to the velocity measurements. The noisy measurements were low pass filtered using a type II Chebyshev filter before being used in the algorithm. This type of filter was used due to its low group delay. Fig. 6 shows the results of the tracking algorithm when the measurement noise intensity is 0.05. Table I shows the MSE values for Case 1a and Case 1b along with the standard deviation of the noise ( $\sigma$ ) associated with each case. The mean flow velocity of the flow within the tank boundaries was 1.629 m/s for each case. This indicates that when  $I = 0.05$ , the standard deviation of the noise component is almost 20% of the mean flow velocity. Thus it can be seen that the algorithm performs well even in the presence of significant noise.

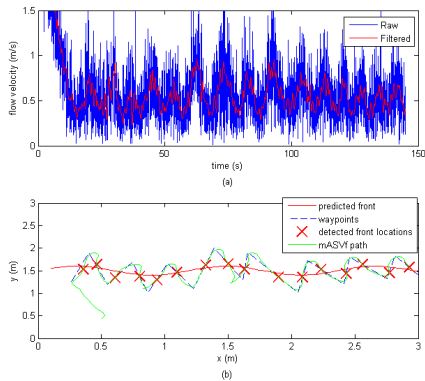


Fig. 6: Tracking a time-invariant velocity front with  $I = 0.05$ . (a) Raw and filtered velocity measurements. (b) Front tracking performance

TABLE I: MSE values for front location detection for Case 1a and Case 1b

Noise Intensity	$\sigma$ (m/s)	MSE (m)
0	0	0
0.01	0.141	0.038
0.05	0.316	0.071

3) *Case 2*: The performance of the algorithm on time varying velocity fronts was tested using the flow field given by (2) with  $A = 0.1$ ,  $\omega_b = \frac{1}{6\pi}$  and  $\omega_m = \frac{1}{\pi}$ . As in the previous case, experiments were conducted for noise intensities 0, 0.01 and 0.05. The results corresponding to  $I = 0.05$  is shown in Fig. 7. The MSE values for Case 2 are shown in Table II. In these experiments, the mean flow velocity of the flow within the tank boundaries was 1.562 m/s. Thus, a noise intensity of  $I = 0.05$  indicates that the standard deviation of the noise component is more than 20% of the mean flow velocity. When these values are compared with the corresponding values for the static case, it can be seen that the algorithm performs almost identically in both cases. This is to be expected because the algorithm makes no assumptions about the location of the front after the first two front locations have been found.

4) *Case 3*: The final experiment conducted used the mASVf with actual flow fields in the MR tank. Fig. 8(a) shows the actual measured velocity and Fig. 8(b) shows the results of the front tracking. The red line indicates the initial front location provided to the initial path generator and the black line indicates the actual front detected by the algorithm. Fig. 4 shows the photograph of the experimental setup where

TABLE II: MSE values for front location detection for Case 2

Noise Intensity	$\sigma$ (m/s)	MSE (m)
0	0	0
0.01	0.141	0.041
0.05	0.316	0.068

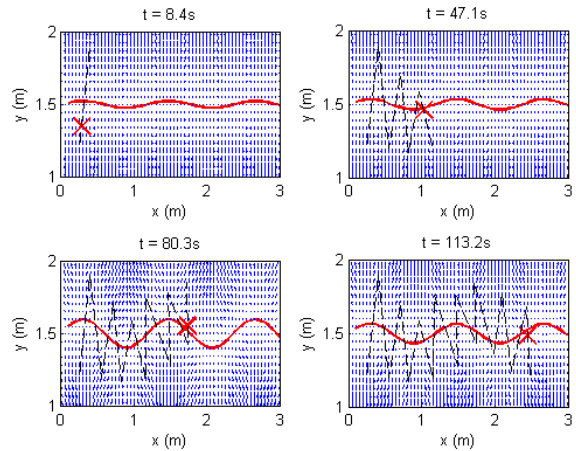


Fig. 7: Tracking a time varying velocity front with  $I = 0.05$ .

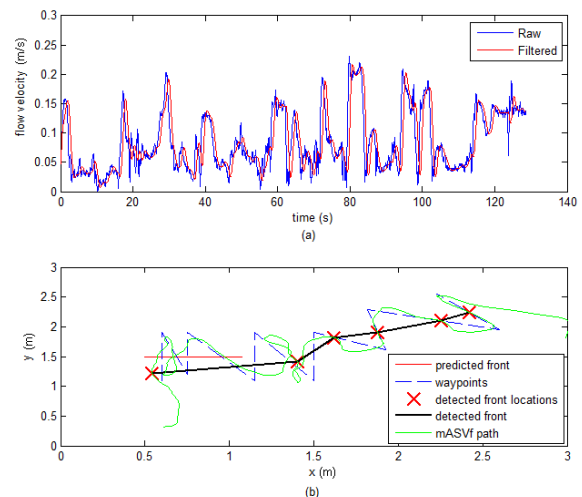


Fig. 8: Tracking a velocity front in an actual flow in the MR tank. (a) Raw and filtered velocity measurements. (b) Front tracking performance

white pellets have been used to visualize the front location. On comparison of the two figures, it can be seen that the algorithm provides a reasonable approximation of the actual velocity front. Currently a method is not available to detect the actual front locations in the MR tank accurately. Hence, it is not possible to provide a quantitative measure of the performance of the algorithm when actual flows are generated in the MR tank. This is a direction for future work.

## VI. CONCLUSIONS AND FUTURE WORK

In this paper we have developed an algorithm to track various fronts in an aquatic environment. We have successfully tested and validated the algorithm on a variety of test cases where the algorithm was used to track a velocity front using a novel testbed capable of creating controllable fluidic features in a laboratory setting. The main advantage of this algorithm is its simplicity and the associated ease of implementation.

In spite of its simplicity, we have demonstrated that the algorithm is robust to measurement noise. However, some drawbacks were also observed during experimentation. One main drawback of the algorithm is that it will eventually lose track of a front which has a continuous curvature in the same direction; e.g., a circular front. This effect is exacerbated if the curvature of the front is high. This could potentially be overcome by adjusting the parameter  $a$  in the algorithm, depending on which side of the curvature the agent is on. If the agent is heading ‘out’ of the curvature,  $a$  could be increased and if the agent is heading ‘in’ to the curvature,  $a$  could be decreased. Additionally, we are also examining the integration of model predictions to inform the vehicle of frontal movements prior to starting the survey, or predicting frontal evolution during the execution of the mission. This will enable a longer horizon for path planning to place the vehicle in the *right place at the right time* to sample the entire front. Similar to [7], [8] the use of ocean model data for validation through simulations will aid in our progression to full-scale field deployments, but also serves as a valuable intermediary for model testing in the mCoStE.

#### REFERENCES

- [1] Y. Zhang, M. A. Godin, J. G. Bellingham, and J. P. Ryan, “Using an Autonomous Underwater Vehicle to Track a Coastal Upwelling Front,” *IEEE Journal of Oceanic Engineering*, vol. 37, no. 3, pp. 338–347, July 2012.
- [2] D. Olson, G. Hitchcock, A. Mariano, C. Ashjan, G. Peng, R. Nero, and G. Podesta, “Life on the edge: marine life and fronts,” *Oceanography*, vol. 7, pp. 52–60, 1994.
- [3] I. M. Belkin and J. E. O’Reilly, “An algorithm for oceanic front detection in chlorophyll and SST satellite imagery,” *Journal of Marine Systems*, vol. 78, pp. 319–326, 2009.
- [4] A. G. P. Shaw and R. Vennell, “A Front-Following Algorithm for AVHRR SST imagery,” *Remote Sensing of Environment*, vol. 72, pp. 317–327, 2000.
- [5] G. Haller and G. Yuan, “Lagrangian coherent structures and mixing in two-dimensional turbulence,” *Phys. D*, vol. 147, pp. 352–370, December 2000. [Online]. Available: <http://dl.acm.org/citation.cfm?id=366463.366505>
- [6] R. N. Smith, P. Cooksey, F. Py, G. S. Sukhatme, and K. Rajan, “Adaptive path planning for tracking ocean fronts with an autonomous underwater vehicle,” in *International Symposium on Experimental Robotics (ISER 2014)*, Marrakech/Essaouira, Morocco, June 2014.
- [7] B. Reed and F. Hover, “Oceanographic pursuit: Networked control of multiple vehicles tracking dynamic ocean features,” *Methods in Oceanography*, pp. 1–23, May 2014. [Online]. Available: <http://linkinghub.elsevier.com/retrieve/pii/S221112201400022X>
- [8] B. L. Reed and F. S. Hover, “Tracking ocean fronts with multiple vehicles and mixed communication losses,” in *Intelligent Robots and Systems (IROS), 2013 IEEE/RSJ International Conference on*, Nov. 2013, pp. 3374–3381.
- [9] R. N. Smith, M. Schwager, S. L. Smith, B. H. Jones, D. Rus, and G. S. Sukhatme, “Persistent Ocean Monitoring with Underwater Gliders: Adapting Sampling Resolution,” *Journal of Field Robotics*, vol. 28, no. 5, pp. 714–741, 2011. [Online]. Available: [http://cres.usc.edu/cgi-bin/print\\\_pub\\\_details.pl?pubid=710](http://cres.usc.edu/cgi-bin/print\_pub\_details.pl?pubid=710)
- [10] R. N. Smith, J. Das, H. Heidarsson, A. Pereira, I. Cetinić, L. Darjany, M.-E. Garneau, M. D. Howard, C. Oberg, M. Ragan, A. Schnetzer, E. Seubert, E. C. Smith, B. A. Stauffer, G. Toro-Farmer, D. A. Caron, B. H. Jones, and G. S. Sukhatme, “{USC} {CINAPS} Builds Bridges: Observing and Monitoring the {S}outhern {C}alifornia {B}ight,” *IEEE Robotics and Automation Magazine, Special Issue on Marine Robotics Systems*, vol. 17, no. 1, pp. 20–30, Mar. 2010.
- [11] R. N. Smith, Y. Chao, P. P. Li, D. A. Caron, B. H. Jones, and G. S. Sukhatme, “Planning and Implementing Trajectories for Autonomous Underwater Vehicles to Track Evolving Ocean Processes based on Predictions from a Regional Ocean Model,” *International Journal of Robotics Research*, vol. 29, no. 12, pp. 1475–1497, Oct. 2010. [Online]. Available: [http://cres.usc.edu/cgi-bin/print\\\_pub\\\_details.pl?pubid=646](http://cres.usc.edu/cgi-bin/print\_pub\_details.pl?pubid=646)
- [12] R. N. Smith, A. Pereira, P. P. Li, D. A. Caron, B. H. Jones, and G. S. Sukhatme, “Autonomous Underwater Vehicle trajectory design coupled with predictive ocean models: A case study,” in *2010 IEEE International Conference on Robotics and Automation*. IEEE, 2010, pp. 4770–4777. [Online]. Available: <http://ieeexplore.ieee.org/lpdocs/epic03/wrapper.htm?arnumber=5509240>
- [13] E. L. Creed, C. Mudgal, S. Glenn, O. Schofield, C. Jones, and D. C. Webb, “Using a Fleet of Slocum Battery Gliders in a Regional Scale Coastal Ocean Observatory,” in *Oceans ’02 MTS/IEEE*, 2002.
- [14] E. Fiorelli, N. E. Leonard, P. Bhatta, D. A. Paley, R. Bachmayer, and D. M. Fratantoni, “Multi-AUV Control and Adaptive Sampling in Monterey Bay,” *Oceanic Engineering, IEEE Journal of*, vol. 31, no. 4, pp. 935–948, Oct. 2006.
- [15] Y. Zhang, M. Godin, J. G. Bellingham, and J. P. Ryan, “Ocean front detection and tracking by an autonomous underwater vehicle,” in *MTS/IEEE Oceans 2011*, Sept. 2011, pp. 1–4.
- [16] Y. Zhang, J. G. Bellingham, J. P. Ryan, B. Kieft, and M. J. Stanway, “Two-dimensional mapping and tracking of a coastal upwelling front by an autonomous underwater vehicle,” in *MTS/IEEE Oceans - San Diego*, Sept. 2013, pp. 1–4.
- [17] I. M. Belkin, P. C. Cornillon, and K. Sherman, “Fronts in Large Marine Ecosystems,” *Progress In Oceanography*, vol. 81, no. 1-4, pp. 223–236, 2009.
- [18] N. E. Leonard, D. A. Paley, R. E. Davis, D. M. Fratantoni, F. Lekien, and F. Zhang, “Coordinated control of an underwater glider fleet in an adaptive ocean sampling field experiment in Monterey Bay,” *Journal of Field Robotics*, vol. 27, no. 6, pp. 718–740, 2010. [Online]. Available: <http://dx.doi.org/10.1002/rob.20366>
- [19] J. Das, T. Maughan, M. McCann, M. Godin, T. O’Reilly, M. Messie, F. Bahr, K. Gomes, F. Py, J. Bellingham, G. Sukhatme, and K. Rajan, “Towards mixed-initiative, multi-robot field experiments: Design, deployment, and lessons learned,” in *Proceedings of the Intelligent Robots and Systems (IROS) Conference*, San Francisco, 2011.
- [20] G. A. Hollinger and G. S. Sukhatme, “Trajectory Learning for Human-robot Scientific Data Collection,” in *IEEE International Conference on Robotics and Automation*, no. Section V, Hong Kong, May 2014, pp. 1–6.
- [21] C. Hsieh, Z. Jin, D. Marthaler, B. Nguyen, D. Tung, A. Bertozzi, and R. Murray, “Experimental validation of an algorithm for cooperative boundary tracking,” in *Proc. of the 2005 American Control Conference.*, 2005, pp. 1078–1083.
- [22] S. Susca, S. Martinez, and F. Bullo, “Monitoring environmental boundaries with a robotic sensor network,” *IEEE Transactions on Control Systems Technology*, vol. 16, no. 2, pp. 288–296, 2008.
- [23] I. Triandaf and I. B. Schwartz, “A collective motion algorithm for tracking time-dependent boundaries,” *Mathematics and Computers in Simulation*, vol. 70, pp. 187–202, 2005.
- [24] V. M. Goncalves, L. C. A. Pimenta, C. A. Maia, B. Dutra, and G. A. S. Pereira, “Vector fields for robot navigation along time-varying curves in n-dimensions,” *IEEE Transactions on Robotics*, vol. 26, no. 4, pp. 647–659, 2010.
- [25] F. Zhang, D. M. Fratantoni, D. Paley, J. Lund, and N. E. Leonard, “Control of coordinated patterns for ocean sampling,” *International Journal of Control*, vol. 80, no. 7, pp. 1186–1199, 2007.
- [26] W. Wu and F. Zhang, “Cooperative exploration of level surfaces of three dimensional scalar fields,” *Automatica, the IFAC Journal*, vol. 47, no. 9, pp. 2044–2051, 2011.
- [27] M. Michini, M. A. Hsieh, E. Forgoston, and I. B. Schwartz, “Robotic tracking of coherent structures in flows,” *IEEE Trans. on Robotics*, vol. 30, no. 3, pp. 593–603, 2014.
- [28] D. Larkin, M. Michini, A. Abad, S. Teleski, and M. A. Hsieh, “Design of the multi-robot coherent structure testbed (mcoSte) for distributed tracking of geophysical fluid dynamics,” in *ASME International Design Engineering Technical Conferences (IDETC)*, Buffalo, NY USA, Aug 2014.
- [29] G. Veronis, “Wind-driven ocean circulation, part i and part ii,” *Deep-Sea Res.*, vol. 13, no. 31, 1966.